



## Easy, fast, and clean fluorescence analysis of tryptophan with clays and graphene/clay mixtures

Lucía Gutiérrez Fernández<sup>a</sup>, Soledad Vera-López<sup>a,b</sup>, Ana María Díez-Pascual<sup>a,b</sup>,  
María Paz San Andrés<sup>a,b,\*</sup>

<sup>a</sup> Universidad de Alcalá, Facultad de Ciencias, Departamento de Química Analítica, Química Física e Ingeniería Química, Ctra. Madrid-Barcelona Km. 33.6, 28805 Alcalá de Henares, Madrid, Spain

<sup>b</sup> Universidad de Alcalá, Instituto de Investigación Química Andrés M. del Río (IQAR), Ctra. Madrid-Barcelona Km. 33.6, 28805 Alcalá de Henares, Madrid, Spain

### ARTICLE INFO

#### Keywords:

Bentonite  
Sepiolite  
Graphene  
Tryptophan  
Fluorescence  
Dispersive solid phase extraction

### ABSTRACT

Clays (C) such as sepiolite (SEP) or bentonite (BEN) and their mixtures with graphene (G) have been used as sorbents in dispersive solid phase extraction (dSPE). Tryptophan (TRP) analysis by fluorescence combined with a sample preparation step using G/C 30/70 w/w mixture provides a quantitative TRP retention, independently of the amino acid concentration with a desorption process feasible in 80 mM aqueous solution of the surfactant Brij L23. Under these conditions, the detection and quantification limits are 3.5 and 11.8  $\mu\text{g L}^{-1}$ , respectively. Additionally, a novel, simple and inexpensive method has been developed to directly analyse TRP in real samples, in which the presence of matrix interferents typically limits to obtain accurate results. For the first time, BEN has been used as an effective clean-up sorbent for the fluorimetric analysis of TRP in beer, leading to results without statistical differences versus those of a reference HPLC method free of interferences, with recoveries of 90 % and 100 %. The proposed method can be applied to accurately analyse TRP in complex matrices in a direct, easy, fast and sustainable way.

### 1. Introduction

Tryptophan (TRP) is an essential hydrophobic amino acid, precursor for bioactive compounds such as vitamin B<sub>6</sub>, serotonin, a neurotransmitter crucial in controlling appetite, sleep, mood, and pain, as well as melatonin, a strong antioxidant and anti-inflammatory agent considered as a therapeutic adjuvant for COVID-19 handling (Reiter et al., 2020). Dietary TRP and its metabolites contribute to the therapy of autism, cardiovascular disease, cognitive function, depression, inflammatory bowel disease, multiple sclerosis, microbial infections and so forth (Markus et al., 2008). It also enables the diagnosis of illnesses such as human cataracts, colon neoplasms, renal cell carcinoma and diabetic nephropathy (Gakamsky et al., 2011).

TRP cannot be analyzed by standard amino acid analysis methods, hence alternative procedures to quantify TRP in foods like dietary supplements are pursued (Friedman, 2018). In this regard, different analytical methods including the use of acid ninhydrin, near-infrared reflectance spectroscopy, colorimetry, and high-performance liquid

and gas chromatography-mass spectrometry have been developed (Palomino-Vasco et al., 2019; Poveda, 2019). Besides, novel detection tools have been recently the focus of thorough research since provide improved signal-to-noise ratio, high specificity and sensitivity, and broad dynamic range (Wu et al., 2018; Ritota and Manzi, 2020). Nonetheless, some of these methods are expensive and/or time-consuming and have complicated analysis systems. Therefore, there is still a need to develop simple, sustainable and low-cost approaches for TRP determination.

This amino acid is the most abundant constituent of proteins, with a maximum UV absorbance at  $\sim 280$  nm and emission at  $\sim 360$  nm, which depend on the polarity of the medium and its microenvironment (Eftink, 2006). When TRP is present on the protein surface, the fluorescence is higher compared to when it is inside the protein (Ghisaidobe and Chung, 2014; Chen et al., 2014). Therefore, this technique can be used to determine the conformational state of a protein and its folding process. TRP is positively charged at  $\text{pH} < \text{pK}_{a1}$  (2.5), while it is negatively charged at  $\text{pH} > \text{pK}_{a2}$  (9.4) (Fig. S1). The fluorescence of TRP is

\* Corresponding author at: Universidad de Alcalá, Facultad de Ciencias, Departamento de Química Analítica, Química Física e Ingeniería Química, Ctra. Madrid-Barcelona Km. 33.6, 28805 Alcalá de Henares, Madrid, Spain.

E-mail address: [mpaz.sanandres@uah.es](mailto:mpaz.sanandres@uah.es) (M.P. San Andrés).

<https://doi.org/10.1016/j.jfca.2022.104858>

Received 11 May 2022; Received in revised form 15 July 2022; Accepted 22 August 2022

Available online 25 August 2022

0889-1575/© 2023 The Authors. Published by Elsevier Inc. This is an open access article under the CC BY-NC-ND license (<http://creativecommons.org/licenses/by-nc-nd/4.0/>).

pH-dependent, thus it has been used as a fluorescent probe in numerous studies (Ghisaidobe and Chung, 2014). Fluorescence is very sensitive, though it suffers from matrix interferences in real samples. As a result, chromatographic separation prior to fluorescence measurements is required to isolate the TRP analyte (Boulet et al., 2017).

Different organic solvents (Chao et al., 2019) and ionic liquids (Li et al., 2013; Zeinali et al., 2017) have been used to extract TRP from complex matrices. In this regard, solid phase extraction (SPE) is an effective way to isolate TRP from food samples (Abdolmohammad-Zadeh and Oskoyi, 2015; Pranil et al., 2021). Dispersive solid-phase extraction (dSPE) is an alternative technique to solid phase extraction introduced by Anastassiades (Anastassiades et al., 2003). It consists of adding the sorbent to the liquid sample followed by shaking and centrifugation to ensure that the analytes are retained. It requires no conditioning or washing steps, hence it is faster and simpler than the SPE method. The sorbent selection in SPE and dSPE is crucial to achieve high selectivity. Numerous materials have been tested as sorbents including molecularly imprinted polymers (MIPs), layered double hydroxides (LDHs), metallic organic frameworks (MOFs), magnetic nanoparticles and carbon nanomaterials (Scigalski and Kosobucki, 2020; Zhang et al., 2022; Han et al., 2022; Han et al., 2021; Li et al., 2020). Fullerenes, quantum dots (QDs), carbon nanotubes (CNTs), graphene (G) and its derivatives graphene oxide (GO) or its mixtures with silica (Azzouz et al., 2018; Benítez-Martínez and Valcárcel, 2015; González-Sálamo et al., 2016; Cui et al., 2020; de Toffoli et al., 2018; Zolfonoun, 2019; Niu et al., 2018) have been used as sorbents due to their high specific surface area for analyte adsorption. In most of the abovementioned studies, organic solvents like methanol, ethanol, acetonitrile, acetone, chloroform, and so forth were used as eluents. However, alternative environmentally friendly reagents are pursued to make the process greener and safer. In this regard, the use of surfactants has many advantages including low cost and lower toxicity, good selectivity, and high solubilization capacity (Yazdi, 2011). Our research group has recently reported the use of surfactant solutions in dSPE for the desorption of riboflavin from sepiolite (Mateos et al., 2018) and of polycyclic aromatic hydrocarbons from graphene/sepiolite mixtures (Mateos et al., 2019).

Clays such as sepiolite (SEP) and bentonite (BEN), with high porosity and intercalation capacity, are ideal nanometric sorbents in dSPE, either alone or mixed with other nanomaterials such as G. SEP is a natural hydrated magnesium silicate with fibrous morphology and a crystal structure comprising talc-like ribbons set parallel to the fiber direction (Frydrych et al., 2011). It has very high cation-exchange capacity and microporosity, resulting in tunnels in which organic molecules can be retained as well as in the clay surface via interaction with the silanol groups (Aranda et al., 2018). On the other hand, BEN is composed of octahedral sheets of aluminum and tetrahedral sheets of silica (Khoieini et al., 2009). Each unit cell consists of an octahedral sheet of aluminum sandwiched between two sheets of tetrahedral silica.

In this work, simple and fast TRP determination has been performed for the first time based on dSPE using G/SEP or G/BEN mixtures as solid sorbents, followed by fluorimetric detection. For such purpose, surfactant aqueous solutions were chosen as green, non-toxic and inexpensive agents for TRP desorption. The extraction of interferents but not TRP using pure BEN has been applied to the direct quantification of TRP in beer samples, and no statistically differences were found with the results obtained by a HPLC reference method.

## 2. Materials and methods

### 2.1. Chemicals and reagents

High purity sepiolite (>95 %), with composition of (wt): 60.2 % SiO<sub>2</sub>, 1.7 % Al<sub>2</sub>O<sub>3</sub>, 0.7 % Fe<sub>2</sub>O<sub>3</sub>, 0.4 % CaO, 26.1 % MgO, 0.1 % Na<sub>2</sub>O and 0.3 % K<sub>2</sub>O, particle size smaller than 75 μm and a specific surface area of 290 m<sup>2</sup> g<sup>-1</sup> and high purity bentonite, were supplied by Sepiol SA (Azuqueca de Henares, Spain). AvanGRAPHENE, G powder with

lamellar structural morphology comprising less than 6 layers with a thickness ≤2 nm and a specific surface area of 480 m<sup>2</sup> g<sup>-1</sup> was provided by Avanzare Innovación Tecnológica, SL (Logroño, Spain). Tryptophan (99–101 %, M<sub>w</sub> = 204.23 g mol<sup>-1</sup>) was obtained from Sigma (Madrid, Spain). The surfactant polyoxyethylene-23-lauryl ether (Brij L23, C<sub>12</sub>H<sub>25</sub>(OCH<sub>2</sub>CH<sub>2</sub>)<sub>23</sub>OH, M<sub>w</sub> = 1198.56 g mol<sup>-1</sup>, CMC = 91 μM) was purchased from Sigma (Madrid, Spain). Hexadecyltrimethylammonium bromide (CTAB, C<sub>19</sub>H<sub>42</sub>BrN, M<sub>w</sub> = 364.46 g mol<sup>-1</sup>, CMC = 0.9 mM) was obtained from Merck (Darmstadt, Germany). Potassium dihydrogen Phosphate (KH<sub>2</sub>PO<sub>4</sub>, 99.5 %, M<sub>w</sub> = 136.09 g mol<sup>-1</sup>) was obtained from Scharlab (Barcelona, Spain) and sodium hydroxide (NaOH, 99 %, M<sub>w</sub> = 40.00 g mol<sup>-1</sup>) was obtained from Merck (Darmstadt, Germany). All the reagents were of analytical grade and were used without further purification. All the aqueous solutions were prepared using ultrapure water obtained from a Milli-Q system (Millipore, Milford, USA).

A stock solution of tryptophan (20 mg L<sup>-1</sup>) was prepared by weighing the appropriate amount and filling up to 100 mL with ultrapure water. Phosphate buffer solution were prepared by weighing the amount of KH<sub>2</sub>PO<sub>4</sub> to obtain a 0.01 M concentration and adjusting the pH with NaOH 0.5 M. All solutions were stored at 4°C under dark conditions.

Low alcohol beer samples (1 % v/v) supplied in 330 mL cans were purchased in a local market (Alcalá de Henares, Spain) and used as received.

### 2.2. Instrumental

Fluorescence spectra were recorded at 25 ± 1°C with a PerkinElmer LS-50B luminescence spectrophotometer (Perkin-Elmer, Massachusetts, USA) equipped with a Xe flash lamp and quartz cuvettes of 1 cm path length thermostatised with a Braun Thermomix BU bath (Analytical Instruments LLC, Minneapolis, USA). The excitation and emission slit widths were 5 nm, and the scan speed was 500 nm min<sup>-1</sup>. The acquisition and data analysis were carried out using the Perkin-Elmer FLWin Lab software.

Reverse phase high performance liquid chromatography (RP-HPLC) measurements were carried out on a chromatographic system equipped with a binary LC pump Flexar with vacuum degasification (Perkin-Elmer, Massachusetts, USA), a manual six-port Rheodyne injection valve with a 20 μL loop, a Jet-Stream Plus column thermostat (Knauer, Berlin, Germany), and a 200 series programmable fluorescence detector (Perkin-Elmer, Massachusetts, USA). The acquisition and processing of the chromatographic data was carried out using TotalChrom WS software (Perkin-Elmer, Massachusetts, USA). The analytical column was Chromaphase RP-18 (5 μm, 150 × 4.6 mm), from Scharlab (Barcelona, Spain). The mobile phase was MeOH/H<sub>2</sub>O 30/70 v/v with a flow of 1 mL min<sup>-1</sup> at 25 °C. The tryptophan peak appears at a retention time of 3.0 min without interferences.

pH values were measured using a WTW InoLab pH-meter (Mexico DF, Mexico). A Vibromatic mechanical stirrer (Selecta, Barcelona, Spain) was used for shaking the mixtures that were centrifuged using a Digicen refrigerated centrifuge (Ortoalresa, Madrid, Spain).

Tip sonication was performed with a UP400S ultrasonic probe system (Hielscher Ultrasonics GmbH, Teltow, Germany), incorporating a titanium sonotrode of 3 mm diameter and approx 100 mm length.

Transmission electron microscopy (TEM) images were acquired using a Zeiss EM-10 C/CR instrument (Oberkochen, Germany) operating at a voltage of 60 kV, with a magnification of 50.000×.

Scanning Electron Microscopy (SEM) micrographs were obtained with a Zeiss DSM-950 SEM (Oberkochen, Germany), operating at an acceleration voltage of 15.0 kV, with a magnification of 20.000×.

Statistical analysis was carried out using the Statgraphics Centurion XVII version 17.0.16.

## 2.3. Procedure

### 2.3.1. Analysis of tryptophan by fluorescence in aqueous solutions

TRP solutions of  $80 \mu\text{g L}^{-1}$  were prepared in phosphate buffer at different pH, and their fluorescence contour graphs were recorded in order to determine the maximum excitation and emission wavelengths and the fluorescence intensity (F). The spectra of TRP were also recorded in surfactant aqueous solutions of CTAB and Brij L23, which were tested as desorbing agents.

The calibration curves in buffer solutions at pH 6 and pH 10 as well as in Brij L23 aqueous solutions were obtained at the maxima excitation and emission wavelengths.

The validation of the method was carried out by the external standard method. The sensitivity, limit of detection (LOD), limit of quantification (LOQ), robustness, linear range and precision were determined using the fluorescence method alone as well as combined with the dSPE process, using Brij L23 as desorbent. The sensitivity was calculated as the slope of the calibration curve, and the LOD and LOQ as the concentration corresponding to the intercept plus three or ten times the standard deviation of the intercept, respectively. The robustness was determined as the relative standard deviation of the slopes obtained in 4 different days. The repeatability (intra-day precision) and reproducibility (inter-day precision) were calculated as the relative standard deviation of 4 measurements performed in the same day and in different days, respectively.

### 2.3.2. Preparation of the graphene/clay mixtures

Mixtures of 100 mg with Graphene/Clay (G/C) weight ratios of 2/98, 4/96, 10/90, 20/80 and 30/70 (w/w) were prepared in order to obtain materials with different polarities. For such purpose, the appropriate amounts of both solids were weighed and mixed in 50 mL of water, subsequently dispersed via sonication with an ultrasonic probe system at 160 W for 10 min, centrifuged at 2598g for 5 min, and finally filtered with a  $0.45 \mu\text{m}$  cellulose filter. The solids were dried at room temperature and preserved for the extractions. A schematic representation of the whole synthesis process of the G/C mixtures is depicted in Fig. S2.

### 2.3.3. Tryptophan extraction with graphene/clay mixtures as sorbents

The extraction process was initially carried out by mixing 10 mg of the G/C solid with 25 mL of a TRP solution ( $80 \mu\text{g L}^{-1}$ ). The mixture was shaken by mechanical agitation for 15 min and subsequently centrifuged for 5 min at 2598g. Once the supernatant was separated, it was measured by fluorescence at 280/360 nm. The TRP retained was determined as difference between the final measured concentration and the initial one.

The tube containing the solid after separation from the supernatant was shaken for 15 min with the desorption solution (CTAB or Brij L23) and centrifuged under the same conditions as those of the extraction step. Finally, the supernatant was measured by fluorescence at 280/360 nm.

### 2.3.4. Removal of interferences using pure clays in real samples

TRP concentration in beer samples was determined by direct fluorescence measurements following the dSPE process. The removal of the interferences found in the beer samples was carried out with 20 mg of either pure SEP or BEN, to compare both sorbents that do not retain TRP. A solution with  $80 \mu\text{L}$  or  $120 \mu\text{L}$  of beer diluted in 25 mL of the phosphate buffer at pH 10 was measured by fluorescence and by a reference HPLC method that separates the interferences and TRP. Subsequently, the solution was mixed with the pure clays and shaken via mechanical agitation for 15 min. After centrifugation at 2598g for 5 min, the supernatant was separated and measured by fluorescence and HPLC. The results obtained from both methods were compared by a linear regression statistical comparison. The samples were spiked with  $20 \mu\text{g L}^{-1}$  and  $40 \mu\text{g L}^{-1}$  of TRP in order to determine the accuracy of the method.

### 2.3.5. Electron microscopy

The neat clays and the 10/90, 20/80 and 30/70 (w/w) G/C mixtures were observed by transmission electron microscopy (TEM) and scanning electron microscopy (SEM). For TEM observations, a small portion of the solid sample was grinded and dispersed in water. One drop of the dispersion was deposited on a Cu grid with carbon formvar and was subsequently dried at room temperature. For SEM observations, the solid samples were grinded and fixed with double sided tape on the sample holder. Samples were metalized with an Au thin layer to avoid charging during electron irradiation.

## 3. Results and discussion

### 3.1. Electron microscopy analysis of graphene/clay mixtures

The neat clays and the G/C mixtures were observed by electron microscopy, in order to get insight about the differences in the structure and morphology as the graphene percentage increases. Representative SEM and TEM micrographs are compared in Figs. 1 and 2, respectively.

Neat SEP presents a fibrous morphology, comprising long, straight, needle-like fiber bundles with a smooth surface and diameters in the range of 30–50 nm (Fig. 1a). The images of the G/SEP mixtures reveal a random and uniform dispersion of G sheets within the SEP nanofibers, with very few agglomerates. In the image of the G/SEP 10/90 mixture, the SEP nanofibers appear very close together, forming a compact structure with some graphene layers on their surface (Figs. 1b and 2b). In the images of the G/SEP 20/80 and 30/70 blends, the SEP nanofibers are more separated, forming a less dense and more flexible structure than in pure SEP, and are intercalated and wrapped by the graphene sheets. As the percentage of G in the mixture increases, more G sheets and fewer SEP fibers can be observed, and the degree of dispersion of the graphene sheets improves.

Neat BEN exhibits a lamellar structure built of individual clay nanoplatelets of different sizes, ranging from 100 nm up to more than  $1 \mu\text{m}$  (Fig. 2e). The dark lamellar aggregates joined by coalescence form a flake-shaped structure. In the micrographs of the G/BEN mixtures (Fig. 2f-h, intercalated sheets of both nanomaterials can be clearly observed. The darkest and most rigid areas belong to BEN, while the lightest areas with thinner, flexible and transparent sheets correspond to graphene. As the concentration of G increases, an ordered 3D arrangement comprising intercalated and overlapping sheets of both nanomaterials is formed (Fig. 1h and Fig. 2h), leading to nanocomposites with very high specific surface area, which is beneficial for their use as sorbents in the dSPE process.

### 3.2. Analysis of tryptophan in aqueous media by fluorescence

#### 3.2.1. Spectra of TRP in aqueous media

The fluorescence spectra of TRP in ultrapure water were recorded without adjusting the pH. Fluorescence contour graphs were obtained for TRP concentrations of 10, 20, 40, 50, 60 and  $80 \mu\text{g L}^{-1}$ . Some of these spectra are depicted in Fig. S3. The maximum excitation wavelength for TRP is 280 nm, while the maximum emission wavelength is 360 nm for all the concentrations studied.

The fluorescence of TRP at a concentration of  $80 \mu\text{g L}^{-1}$  was recorded at different pH of the medium. The excitation and emission wavelengths remain constant, though the fluorescence intensity (F) changes strongly upon modifying the pH. Fig. 3 shows the change in F as a function of the pH at 280/360 nm. A nonlinear growth of F is observed, showing a maximum value at pH 10, which indicates that the anionic form is more fluorescent than the zwitterionic and the cationic ones. The extractions were carried out at pH 6, which is around the isoelectric point of TRP, and at pH 10 since it corresponds to the maximum F.

#### 3.2.2. Analytical characteristics of TRP analysis in aqueous media

TRP extractions were performed at pH 6 and 10. The analytical

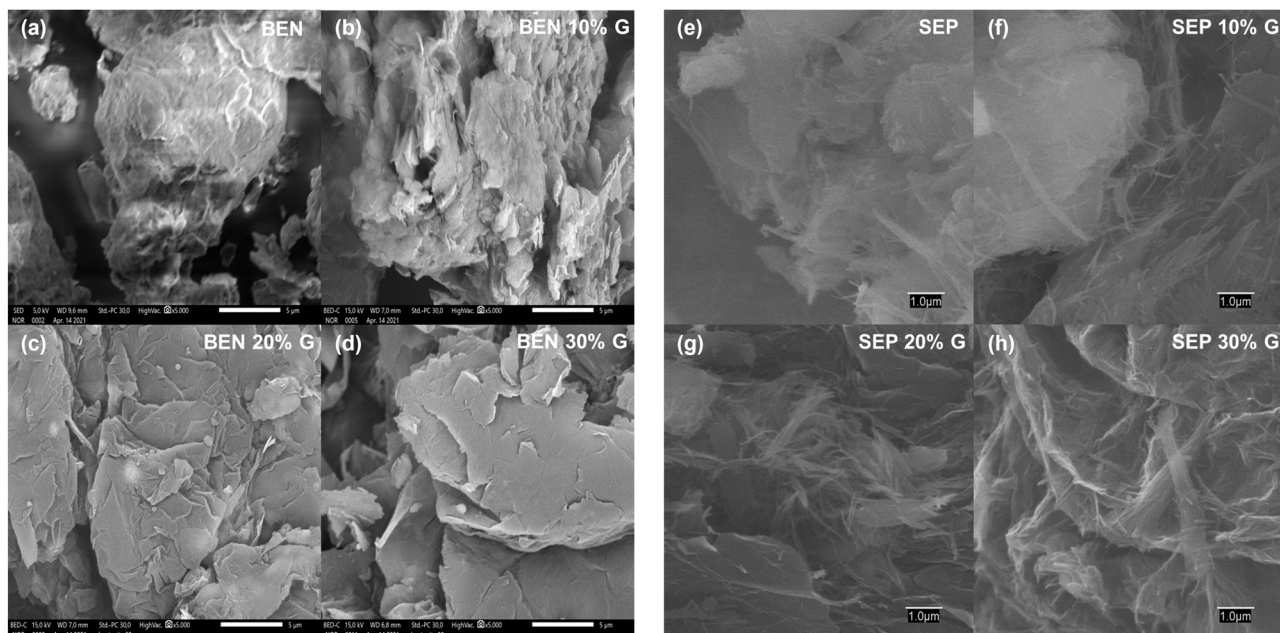


**Fig. 1.** Left: SEM micrographs of bentonite (BEN, a) and G/BEN mixtures 10/90 (b), 20/80 (c) and 30/70 (d) with a magnification of 10,000x. Right: SEM micrographs of sepiolite (SEP, e) and G/SEP mixtures 10/90 (f), 20/80 (g) and 30/70 (h) with a magnification of 5,000x.

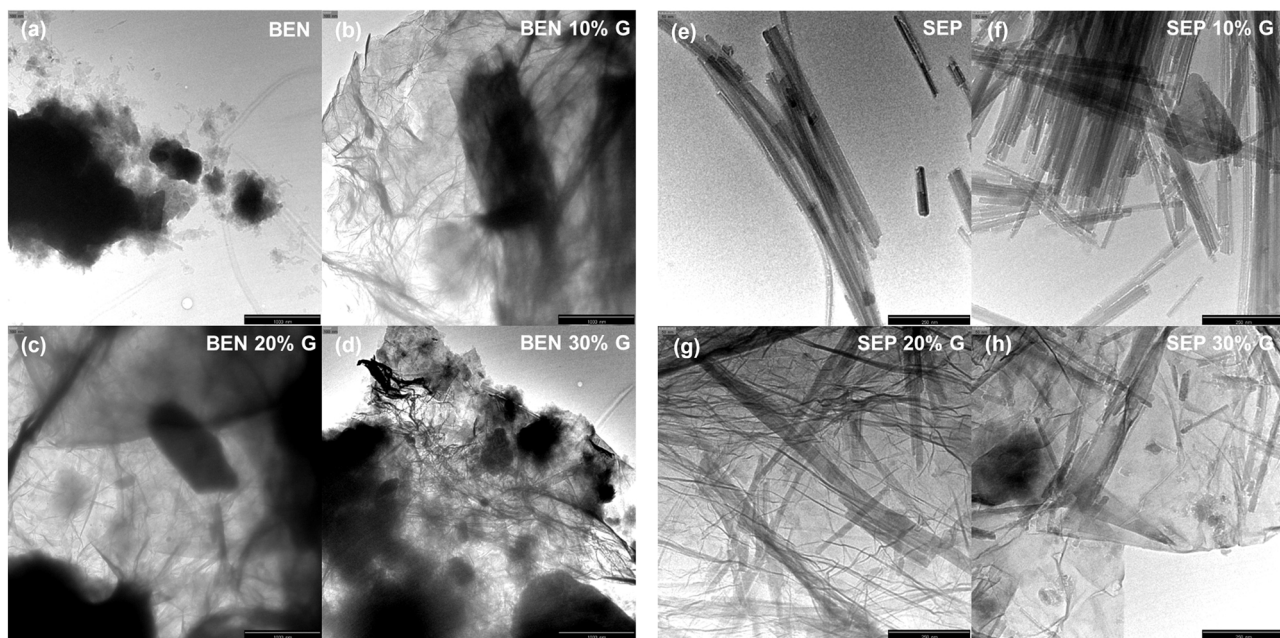


**Fig. 2.** Left: TEM micrographs of bentonite (BEN, a) and G/BEN mixtures 10/90 (b), 20/80 (c) and 30/70 (d) with a magnification of 50,000x. Right: TEM micrographs of sepiolite (SEP, e) and G/SEP mixtures 10/90 (f), 20/80 (g) and 30/70 (h) with a magnification of 10,000x.

characteristics of the fluorescence determination of TRP at both pH are compared in [Table 1](#).

As can be expected, the sensitivity is higher in basic medium due to the higher fluorescence in this pH range. The LOD and LOQ are similar as well as the other characteristics investigated, the robustness and the reproducibility. These values are satisfactory and allow to determine TRP concentrations higher than  $30 \mu\text{g L}^{-1}$ .

### 3.3. Retention of tryptophan in clays and graphene/clay mixtures

TRP retention was studied in different G/C mixtures (from 0/

100–30/70 w/w). At pH 6, TRP concentration was set as  $130 \mu\text{g L}^{-1}$ , and the initial concentrations as well as the concentration in the supernatant after the retention process were determined. For solutions at pH 10, the concentration selected was lower ( $80 \mu\text{g L}^{-1}$ ) due to the higher sensitivity in this medium.

Regarding the pure clays, the retention of TRP at pH 10 is very low, being lower in SEP than in BEN (2.8 % and 16.8 %, respectively). In order to attain higher retention percentage, the neat clays should be mixed with graphene (hydrophobic nanomaterial). The results obtained for the different G/C mixtures at both pH are shown in [Fig. 4](#). As can be observed, for all the graphene percentages studied, the retention in BEN

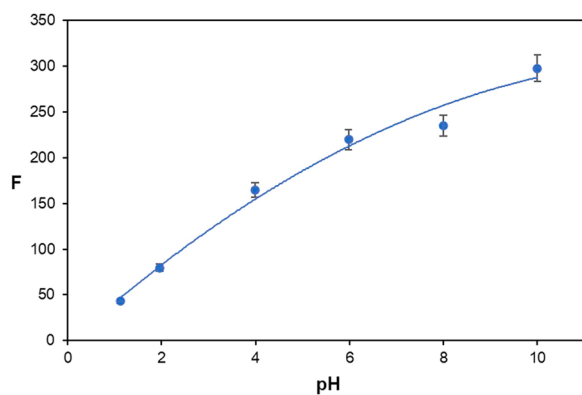


Fig. 3. Change in the fluorescence intensity as a function of pH ( $\lambda_{exc}/\lambda_{em} = 280/360$ ).

Table 1

Analytical characteristics of the fluorescence determination of tryptophan at pH 6 and pH 10.  $\lambda_{exc}/\lambda_{em} = 280/360$  nm.

	pH = 6	pH = 10
Linear Range, $\mu\text{g L}^{-1}$	23–160	30–160
r	0.9991	0.9984
Sensitivity, $\text{L } \mu\text{g}^{-1}$	1.26	2.91
Limit of detection (LOD), $\mu\text{g L}^{-1}$	$7 \pm 4$	$9 \pm 4$
Limit of quantification (LOQ), $\mu\text{g L}^{-1}$	$23 \pm 13$	$30 \pm 12$
Robustness, %RSD* (n = 4)	5.4	8.8
Reproducibility, %RSD* (n = 4)		
[TRP] = $68 \mu\text{g L}^{-1}$	6.85	7.10
[TRP] = $100 \mu\text{g L}^{-1}$	1.44	5.23
[TRP] = $131 \mu\text{g L}^{-1}$	8.09	6.74

\* RSD: Relative Standard Deviation.

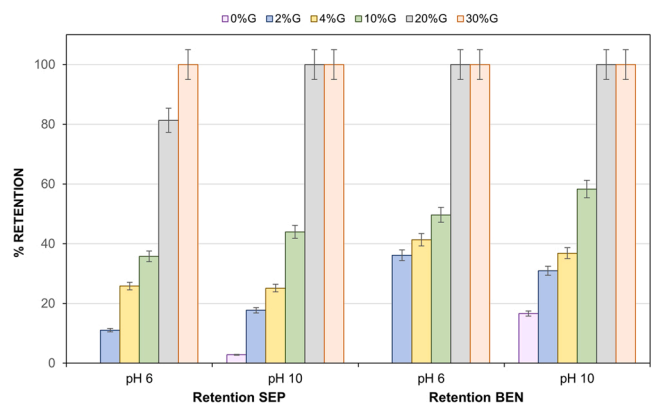


Fig. 4. Comparison of tryptophan (TRP) retention in G/C (Graphene/Clay) mixtures using sepiolite (SEP) or bentonite (BEN) with different composition.

is higher than in SEP, and at pH 10 is higher than at pH 6.

The retention in the mixtures with low graphene percentage (<10 wt. %) is smaller than 50 %, and it increases up to 58 % for G/BEN 10/90 at pH 10. Nonetheless, only the G/C 20/80 and 30/70 mixtures show a retention of 100 %, for both pH in the case of BEN and at pH 10 for SEP. In general, the retention percentage rises with increasing graphene content, and this is ascribed to  $\pi$ - $\pi$  interactions between the solid and TRP, in particular between the  $\pi$  electron cloud of graphene and the aromatic ring of the indole group of the amino acid. Given that the working pH is higher than the  $\text{pK}_{a2}$  (9.4) of TRP, it should be negatively charged (Fig. S1), hence its interaction by H-bonds with the OH groups of the clays should be very weak. Thus, the  $\pi$ - $\pi$  interactions between G and TRP are likely stronger than the hydrogen bonding interactions

between the hydroxyl groups of the clays and the polar groups of TRP. Therefore, a high graphene percentage is required for the quantitative retention of TRP. Considering the abovementioned results, the solid mixtures chosen for the extraction of TRP were G/C 30/70. The photographs of the pure clays, pristine graphene and the G/C 30/70 mixture are shown in Fig. S4.

In addition, the adsorption capacity of TRP on the selected mixture was investigated. Thus, for amino acid concentrations in the range between 20 and  $120 \mu\text{g L}^{-1}$ , a TRP retention of 100 % was attained. For the highest TRP concentration, the adsorption capacity was found to be  $283.7 \mu\text{g g}^{-1}$ .

### 3.4. Desorption of tryptophan from graphene/clay mixtures with surfactant aqueous solutions

The desorption of TRP from the G/C 30/70 in which the retention is quantitative was carried out using aqueous solutions of surfactants of different nature: cationic CTAB and nonionic Brij L23.

#### 3.4.1. Desorption using CTAB

CTAB was used for the desorption of TRP at concentrations ranging between 0.5 and 60 mM. The fluorescence contour graphs of TRP in the CTAB solutions are shown in Fig. S5. As can be observed, the excitation wavelength, emission wavelength and fluorescence intensity are the same to those in phosphate buffer medium. The fluorescence of TRP in the extract obtained with the different CTAB concentrations for SEP and BEN solids is depicted in Fig. S6. The amount desorbed from the solids using CTAB rises with increasing surfactant concentration up to 40 mM, while remains constant at higher concentrations. The highest fluorescence value is obtained at pH 6 for a G/BEN mixture using 40 mM CTAB. The desorption is easier at pH 6 since the retention is weaker than at pH 10, though the TRP recovery is not as high as expected (52.8 %). In addition, the CTAB solutions are difficult to be prepared, due to solid precipitation below  $20^\circ\text{C}$ .

#### 3.4.2. Desorption with Brij L23 solutions

TRP desorption after retention in the G/C mixtures was carried out using Brij L23 concentrations ranging between 20 and 100 mM. Fluorescence contour graphs were recorded for the Brij L23 solutions and the TRP solutions in Brij L23 at different concentrations. Fig. S7 displays the spectra of 20 mM and 100 mM Brij L23 solutions. Despite the most concentrated surfactant solution emits fluorescence within the TRP excitation/emission wavelength range, TRP fluorescence was able to be measured. As shown in Fig. 5, recoveries obtained for Brij L23 concentrations ranging from 20 to 80 mM hardly change. The fluorescence of the amino acid increases when the desorption is performed using 100 mM Brij L23 at pH 10. The analytical characteristics of the fluorescence determination of TRP for the different Brij L23 concentrations are summarized in Table S1.

Brij L23 solutions at a concentration of 100 mM have a high background fluorescence, hence the TRP fluorescence is difficult to be measured. Therefore, 80 mM Brij L23 solution was chosen for TRP recovery subsequently to the retention step performed with G/C 30/70 mixture at pH 10.

### 3.5. Study of the overall retention and recovery extraction method

In order to apply the recovery extraction method, TRP recovery should remain constant upon increasing its concentration. For such purpose, TRP solutions with concentrations ranging between 20 and  $100 \mu\text{g L}^{-1}$  were used, which were retained at pH 10 and desorbed using 80 mM Brij L23 solutions (see Fig. 6). The retention is quantitative (Fig. 6a) and does not depend on the amino acid concentration. However, the recovery (Fig. 6b) is very different in G/BEN solid than in G/SEP. Recovery percentages with G/BEN 30/70 mixture change with increasing TRP concentration, and the maximum value is reached at

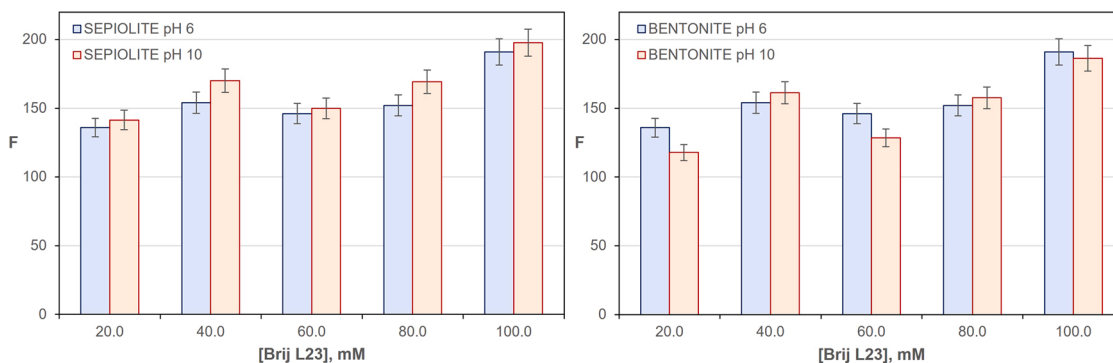


Fig. 5. Change in the fluorescence of the TRP extract ( $80 \mu\text{g L}^{-1}$ ) desorbed with different Brij L23 concentrations.

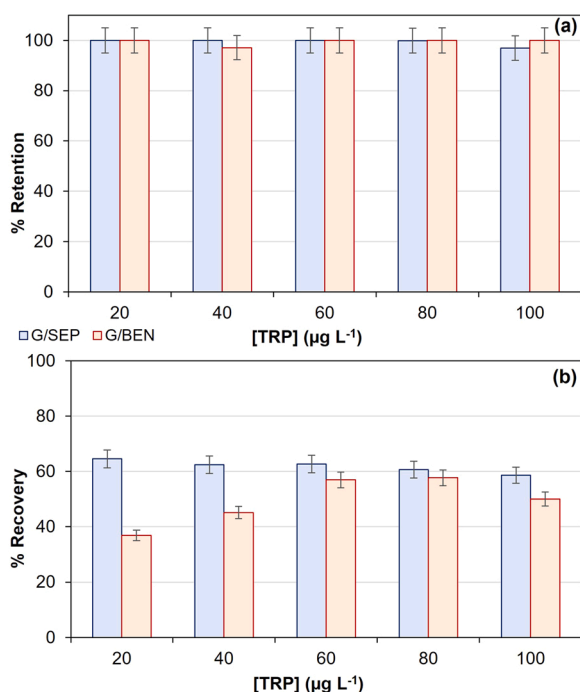


Fig. 6. Change in the recovery for different concentrations of TRP using G/C 30/70 mixture.

$80 \mu\text{g L}^{-1}$ . In the case of G/SEP mixture, the recovery does not depend on the TRP concentration, showing a value close to 60%. Taking into account the above explanations, the selected retention conditions were G/SEP 30/70 mixture at pH 10, and for the recovery, 80 mM Brij L23 aqueous solution.

The validation of the analytical method including the retention and desorption steps of the sample preparation was carried out by determining different analytical parameters. Under the optimal conditions described above, the values obtained are the following: linear range from 12 to  $125 \mu\text{g L}^{-1}$  with a correlation of 0.9991 ( $n = 10$ ), sensitivity of  $0.67 \text{ L } \mu\text{g}^{-1}$  and limit of detection and quantification of  $3.5$  and  $11.8 \mu\text{g L}^{-1}$  respectively. In previous works, different SPE sorbents for TRP extraction have been used. For instance, graphene oxide (GO) with silica ( $\text{GO@SiO}_2$ ) was applied for the analysis of TRP, melatonin and TRP derivatives via HPLC (Niu et al., 2018), and the calculated limit of detection and quantification were found to be  $0.01 \mu\text{g mL}^{-1}$  ( $10 \mu\text{g L}^{-1}$ ) and  $0.25 \mu\text{g mL}^{-1}$  ( $250 \mu\text{g L}^{-1}$ ), respectively. The values obtained in the present work for these two parameters are significantly lower, and the sensitivity calculated in the previous study ( $9.76 \text{ mL } \mu\text{g}^{-1}$ ) is considerably smaller than the one obtained herein ( $0.67 \text{ L } \mu\text{g}^{-1}$ ). In another work focused on TRP analysis by HPLC with fluorescence detection (Islam

et al., 2016), the values of the limit of detection and quantification ( $0.1$  and  $0.34 \text{ mg L}^{-1}$  respectively) are also higher than the ones obtained in this work, as well as higher than the detection limit ( $8.9 \mu\text{g L}^{-1}$ ) attained via SPE with multiwall carbon nanotubes (MWCNT) and fluorescence detection (Zolfonoun, 2019). A lower detection limit ( $0.01 \mu\text{g L}^{-1}$ ) has been obtained using a layered double hydroxide nano-sorbent combined with fluorescence (Abdolmohammad-Zadeh and Oskooyi, 2015), though a preconcentration step was carried out in cartridges which involved a more complex preparation of the sorbent.

The repeatability of the sorbent has been determined for 10 independent determinations at different TRP concentrations (20, 40, 60, 80 and  $100 \mu\text{g L}^{-1}$ ) including the extraction step and analysis by fluorescence, and the result expressed as relative standard deviation (%RSD) is 5.0.

### 3.6. Analysis of beer samples. Study of the removal of the interferences in the direct analysis of tryptophan by fluorescence

In beer samples, TRP content is high enough to be directly measured by fluorescence, which is an easy and fast method that does not consume organic solvents. Thus, these samples were chosen and analysed in order to determine their TRP concentration. However, interference compounds caused a change in the fluorescence signal, hence it did not correspond to that of samples spiked with TRP standard. In the matrix samples, interferent compounds can either increase the fluorescence intensity of TRP or have a quenching effect on it, hence making impossible its direct determination. During the dSPE process performed in this work, these interferences likely retained themselves in the solid, thus inhibiting a good TRP retention, hence modifying both the retention and desorption of this amino acid in the G/SEP 30/70 mixture.

Herein, as an alternative, an analysis by fluorescence combined with dSPE was proposed to measure directly the TRP concentration in a clean-up mode by removing the interferences instead of the TRP extraction and desorption. The results of the TRP retention in the different G/C mixtures reveal that in the absence of G, the amino acid retention in either neat SEP or BEN is low. Therefore, the raw clays can be used in real samples, with the goal of removing the interfering substances, thus allowing the direct determination of the amino acid. The efficiency of SEP and BEN for the removal of interferences in the beer samples was compared. With the aim to elucidate the presence or not of interferences, a reference HPLC method free from interferences was

Table 2

Clean-up extraction using sepiolite and bentonite after TRP measurement by fluorescence and HPLC ( $n = 4$ ).

CLAY	[TRP] ( $\mu\text{g L}^{-1}$ ) FLUORESCENCE	[TRP] ( $\mu\text{g L}^{-1}$ ) HPLC	DIFFERENCE ( $\mu\text{g L}^{-1}$ )
SEPIOLITE	$72 \pm 5$	$49 \pm 3$	23
BENTONITE	$54 \pm 3$	$49 \pm 7$	5

applied and the results compared with the developed fluorescence method. The data obtained from both methods are shown in Table 2.

According to the reference method, the TRP concentration measured directly in the beer samples is  $49 \mu\text{g L}^{-1}$ . This result is in very good agreement with that obtained by fluorescence ( $54 \mu\text{g L}^{-1}$ ) after using BEN as sorbent in the clean-up dSPE process, which indicates that this clay can effectively remove most of the interferences. Conversely, SEP is not able to remove the interferences, since the TRP concentration measured after the clean-up process is  $72 \mu\text{g L}^{-1}$ . Therefore, BEN was chosen to remove the interferences in beer samples, making possible to quantify TRP directly after a simple and fast dSPE process without the use of any solvent.

TRP concentration data obtained using the clean-up step with BEN followed by fluorescence measurements were compared with those obtained using HPLC. In addition, with the aim to evaluate the accuracy of the method, some samples were spiked with a TRP standard of  $20 \mu\text{g L}^{-1}$  and  $40 \mu\text{g L}^{-1}$  and determined by both methods. The values measured before ( $[\text{TRP}]_F$ ) and after ( $[\text{TRP}]_{F(S)}$ ) the removal of interferences as well as the values measured by HPLC are compared in Table 3. As an example, Fig. S8 shows a chromatogram of the TRP standard, and a beer sample.

Measurements were carried out in quadruplicate ( $n = 4$ ) for each variable. Systematically, the values measured before the clean-up extraction are higher than those obtained by HPLC, indicating that there are interferences in the fluorescence method that hinder the direct measurement of TRP. By using a small amount of neat BEN in the extraction step, these interferences can be removed without the need of solvents. The values obtained by fluorescence after the clean-up extraction agree well with those obtained by HPLC, and the TRP recovery is very high, ranging systematically between 90 % and 100 %.

The reproducibility of the sorbent (BEN) for 4 different determinations of TRP in beer expressed as % RSD is 2.1. The RSD for 4 different samples spiked with  $20 \mu\text{g L}^{-1}$  and  $40 \mu\text{g L}^{-1}$  is 2.2 and 0.7, respectively. These values demonstrate the good precision of the method with BEN as sorbent in the clean-up process.

A statistical comparison of the data obtained by fluorescence and HPLC was performed using a linear regression, by plotting the fluorescence data in the Y axis and the HPLC data in the X axis. If both methods are statistically equal, the confidence interval of the intercept at 95 % confidence should comprise the 0 value and the confidence interval of the slope should include the 1 value. Twenty pairs of measurements by both methods were included in the comparison, and the results are shown in Fig. 7. The intercept interval is  $4.2 \pm 9.8$ , which includes the value 0, and the slope is  $0.9 \pm 0.1$ , which includes the value 1. Therefore, the results obtained by both methods are statistically the same.

The greenness of the method has been evaluated according to the Pena-Pereira et al. criteria (Pena-Pereira et al., 2020) with 12 different scores, and the value obtained is 0.65, which can be regarded as a good value since it is located above the middle of the scale. Overall, the developed method can be considered as a green approach.

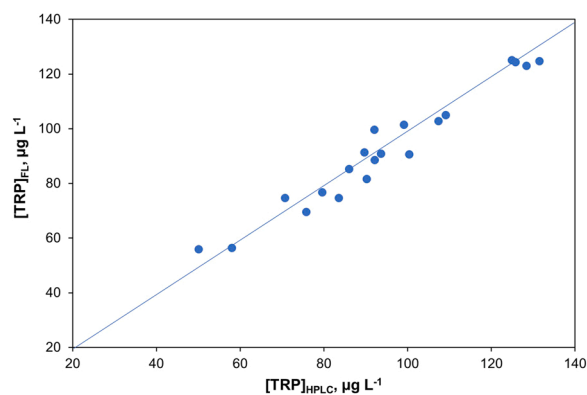


Fig. 7. Comparison of the results obtained by fluorescence after the clean-up process with BEN and by HPLC using a linear regression for a confidence of 95 %.

#### 4. Conclusions

Herein, a novel, simple and inexpensive method for the direct determination of TRP via combination of fluorescence measurements with a dSPE sample preparation step is reported. Graphene/Clay mixtures have been used as sorbents in the dSPE process, and the maximum retention (100 %) is reached for a G percentage of 30 wt. %.

The developed method is based on the  $\pi$ - $\pi$  interactions between the aromatic rings of G and tryptophan at pH 10, at which there is lack of positive charges on the amino acid molecule.

The TRP desorption was carried out using aqueous solutions of surfactants of different nature, CTAB and Brij L23. The optimal extraction conditions for the retention were G/SEP 30/70 mixture at pH 10, and for the desorption 80 mM Brij L23 aqueous solution.

The presence of interferences in real samples results in poor selectivity and low recovery values in the TRP determination. The use of bentonite, a safe, cheap and environmentally friendly clay, in the clean-up step allows to analyse TRP in beer samples via a single, sustainable and fast way using molecular fluorescence spectroscopy.

#### CRedit authorship contribution statement

**Lucía Gutiérrez-Fernández:** Experimentation. **Soledad Vera-López:** Writing – review & editing. **Ana María Díez-Pascual:** Writing – review & editing. **María Paz San Andrés:** Methodology, Writing – original draft, Supervision.

#### Declaration of Competing Interest

The authors declare that they have no known competing financial interests or personal relationships that could have appeared to influence the work reported in this paper.

Table 3

Tryptophan determination in beer samples and spiked with  $20 \mu\text{g L}^{-1}$  and  $40 \mu\text{g L}^{-1}$  of TRP.  $[\text{TRP}]_F$ : TRP concentration determined by fluorescence without clean-up;  $[\text{TRP}]_{F(S)}$ : TRP concentration after clean-up with bentonite measured by fluorescence;  $[\text{TRP}]_{\text{HPLC}}$ : TRP concentration determined by HPLC without clean-up;  $[\text{TRP}]_{\text{HPLC}(S)}$ : TRP concentration in the sample determined by HPLC after clean-up.

Beer sample	$[\text{TRP}]_{\text{added}}$ , $\mu\text{g L}^{-1}$	$[\text{TRP}]_F$ , $\text{mg L}^{-1}$	$[\text{TRP}]_{F(S)}$ , $\text{mg L}^{-1}$	$[\text{TRP}]_{\text{HPLC}}$ , $\text{mg L}^{-1}$	$[\text{TRP}]_{\text{HPLC}(S)}$ , $\text{mg L}^{-1}$	% Difference	% Rec
1	–	$22 \pm 1$	$16.8 \pm 0.8$	$16.7 \pm 0.8$	$15 \pm 2$	9.5	–
	$20 \mu\text{g L}^{-1}$	$29.4 \pm 0.3$	$23 \pm 1$	$24 \pm 1$	$24 \pm 2$	4.1	100.0
	$40 \mu\text{g L}^{-1}$	$33 \pm 1$	$28.2 \pm 0.4$	$33.7 \pm 0.7$	$29 \pm 1$	4.4	90.0
2	–	$21.5 \pm 0.4$	$17.5 \pm 0.4$	$17 \pm 1$	$17 \pm 2$	3.6	–
	$20 \mu\text{g L}^{-1}$	$24.6 \pm 0.2$	$21.3 \pm 0.5$	$21 \pm 1$	$21 \pm 2$	0	90.0
	$40 \mu\text{g L}^{-1}$	$31.5 \pm 0.4$	$25.9 \pm 0.2$	$26.5 \pm 0.6$	$26.6 \pm 0.6$	3.1	100.0

## Data availability

No data was used for the research described in the article.

## Acknowledgments

The authors want to thank the Spanish Ministry of Science and Innovation and Universities (MICIU) for funding the work (Project PGC2018-093375-B-I00). Funding from the Community of Madrid within the framework of the Multiyear Agreement with the University of Alcalá for “Stimulus to Excellence for Permanent University Professors”, Ref. EPU-INV/2020/012 is also acknowledged. The authors also want to thank Belén Marcos and the enterprise SEPIOL SA for providing sepiolite and bentonite clays used in this work.

## Appendix A. Supporting information

Supplementary data associated with this article can be found in the online version at [doi:10.1016/j.jfca.2022.104858](https://doi.org/10.1016/j.jfca.2022.104858).

## References

- Abdolmohammad-Zadeh, H., Oskooyi, S., 2015. Solid-phase extraction of L-tryptophan from food samples utilizing a layered double hydroxide nano-sorbent prior to its determination by spectrofluorometry. *J. Iran. Chem. Soc.* 12, 1115–1122. <https://doi.org/10.1007/s13738-014-0572-x>.
- Anastasiades, M., Lehotay, S.J., Stajnbaher, D., Schenck, F.J., 2003. Fast and easy multiresidue method employing acetonitrile extraction/partitioning and dispersive solid-phase extraction for the determination of pesticide residues in produce. *J. AOAC Int* 86, 412–431. <https://doi.org/10.1093/jaoac/86.2.412>.
- Aranda, P., Darder, M., Wicklein, B., Rytwo, G., Ruiz-Hitzky, E., 2018. Hybrid organic-inorganic interfaces. In: Delville, M.H., Taubert, A. (Eds.), *Clay–Organic Interfaces for Design of Functional Hybrid Materials*. Wiley-VCH Verlag GmbH & Co. KGaA, Weinheim, Germany, pp. 1–84.
- Azzouz, A., Kailasa, S.K., Lee, S.S., Rascón, A.J., Ballesteros, E., Zhang, M., Kim, K., 2018. Review of nanomaterials as sorbents in solid-phase extraction for environmental samples. *Trends Anal. Chem.* 108, 347–369. <https://doi.org/10.1016/j.trac.2018.08.009>.
- Benítez-Martínez, S., Valcárcel, M., 2015. Graphene quantum dots in analytical science. *Trends Anal. Chem.* 72, 93–113. <https://doi.org/10.1016/j.trac.2015.03.020>.
- Boulet, L., Faure, P., Flore, P., Montérmal, J., Ducros, V., 2017. Simultaneous determination of tryptophan and 8 metabolites in human plasma by liquid chromatography/tandem mass spectrometry. *J. Chromatogr. B* 1054, 36–43. <https://doi.org/10.1016/j.jchromb.2017.04.010>.
- Chao, Y., Ding, H., Pang, J., Jin, Y., Li, X., Chang, H., Jiang, W., Chen, G., Han, C., Zhu, W., 2019. High efficient extraction of tryptophan using deep eutectic solvent-based aqueous biphasic systems. *Indian J. Pharm. Sci.* 81 (3), 448–455. <https://doi.org/10.36468/pharmaceutical-sciences.529>.
- Chen, Y.W., Lee, C.H., Huang, Y.T., Pan, Y.J., Lin, S.M., Lo, Y.Y., Lee, C.H., Huang, L.K., Huang, Y.F., Hsu, Y.D., 2014. Functional and fluorescence analyses of tryptophan residues in H<sup>+</sup>-pyrophosphatase of *Clostridium tetani*. *J. Bioenerg. Biomembr.* 46, 127–134. <https://doi.org/10.1007/s10863-013-9532-x>.
- Cui, Y., Ma, H., Liu, D., Li, M., Hao, R., Li, J., Jiang, Y., 2020. Graphene oxide adsorbent-based dispersive solid phase extraction coupled with multi-pretreatment clean-up for analysis of trace ochratoxin A in chicken liver. *Chromatographia* 83, 1307–1314. <https://doi.org/10.1007/s10337-020-03942-8>.
- Eftink, M.R., 2006. Fluorescence techniques for studying protein structure. In: *Methods of Biochemical Analysis*. John Wiley & Sons, Inc, Hoboken, NJ, USA, pp. 127–205.
- Friedman, M., 2018. Analysis, nutrition, and health benefits of tryptophan. *Int. J. Tryptophan Res.* 11, 1–12. <https://doi.org/10.1177/1178646918802282>.
- Frydrych, M., Wan, C., Stengler, R., O’Kelly, K.U., Chen, B., 2011. Structure and mechanical properties of gelatin/sepiolite nanocomposite foams. *J. Mater. Chem.* 21, 9103. <https://doi.org/10.1039/C1JM10788G>.
- Gakamsky, D.M., Dhillon, B., Babraj, J., Shelton, M., Smith, S.D., 2011. Exploring the possibility of early cataract diagnostics based on tryptophan fluorescence. *J. R. Soc. Interface* 8 (64), 1616–1621.
- Ghisaidoobe, A.B.T., Chung, S.J., 2014. Intrinsic tryptophan fluorescence in the detection and analysis of proteins: a focus on Förster resonance energy transfer techniques. *Int. J. Mol. Sci.* 15, 22518–22538. <https://doi.org/10.3390/ijms15122518>.
- González-Sálamo, J., Socas-Rodríguez, B., Hernández-Borges, J., Rodríguez-Delgado, M. A., 2016. Nanomaterials as sorbents for food sample analysis. *Trends Anal. Chem.* 85, 203–220. <https://doi.org/10.1016/j.trac.2016.09.009>.
- Han, L., Qin, P., Zhang, X., Li, M., Li, D., Lu, M., Cai, Z., 2021. MIL-101(Fe)-derived magnetic porous carbon as sorbent for stir bar sorptive-dispersive microextraction of sulfonamides. *Microchim. Acta* 188, 340. <https://doi.org/10.1007/s00604-021-04993-w>.
- Han, L., Liu, X., Zhang, X., Li, M., Li, D., Qin, P., Tian, S., Lu, M., Cai, Z., 2022. Preparation of multivariate zirconia metal-organic frameworks for highly efficient adsorption of endocrine disrupting compounds. *J. Hazard. Mater.* 424, 127559. <https://doi.org/10.1016/j.jhazmat.2021.127559>.
- Islam, J., Shirakawa, H., Nguyen, T.K., Aso, H., Komai, M., 2016. Simultaneous analysis of serotonin, tryptophan and tryptamine levels in common fresh fruits and vegetables in Japan using fluorescence HPLC. *Food Biosci.* 13, 56–59. <https://doi.org/10.1016/j.fbio.2015.12.006>.
- Khoeni, M., Bazgir, S., Tamizifar, M., Nemati, A., Arzani, K., 2009. Investigation of the modification process and morphology of organosilane modified nanoclay. *Ceram* 53, 25.
- Li, C., Li, Z., Wang, A., Yin, J., Wang, J., Li, H., Liu, Q., 2013. Aqueous two phase extraction process of tryptophan based on functionalized ionic liquids. *RSC Adv.* 3, 6356–6361. <https://doi.org/10.1039/C3RA23061A>.
- Li, W., Zhang, J., Zhu, W., Qin, P., Zhou, Q., Lu, M., Zhang, X., Zhao, W., Zhang, S., Cai, Z., 2020. Facile preparation of reduced graphene oxide/ZnFe<sub>2</sub>O<sub>4</sub> nanocomposite as magnetic sorbents for enrichment of estrogens. *Talanta* 208, 120440. <https://doi.org/10.1016/j.talanta.2019.120440>.
- Markus, C.R., Firk, C., Gerhardt, C., Kloek, J., Smolders, G.F., 2008. Effect of different tryptophan sources on amino acids availability to the brain and mood in healthy volunteers. *Psychopharmacology* 201, 107–114. <https://doi.org/10.1007/s00213-008-1254-0>.
- Mateos, R., Vera-López, S., Díez-Pascual, A.M., San Andrés, M.P., 2018. Dispersive solid phase extraction/fluorescence analysis of riboflavin using sepiolite as sorbent. *Appl. Clay Sci.* 163, 279–290. <https://doi.org/10.1016/j.clay.2018.07.033>.
- Mateos, R., Vera-López, S., Saz, M., Díez-Pascual, A.M., San Andrés, M.P., 2019. Graphene/sepiolite mixtures as dispersive solid-phase extraction sorbents for the analysis of polycyclic aromatic hydrocarbons in wastewater using surfactant aqueous solutions for desorption. *J. Chromatogr. A* 1596, 30–40. <https://doi.org/10.1016/j.chroma.2019.03.004>.
- Niu, J., Zhang, X., Qin, P., Yang, Y., Tian, S., Yang, H., Lu, M., 2018. Simultaneous determination of melatonin, L-tryptophan, and two L-tryptophan-derived esters in food by HPLC with graphene oxide/SiO<sub>2</sub> nanocomposite as the adsorbent. *Food Anal. Methods* 11, 2438–2446. <https://doi.org/10.1007/s12161-018-1213-2>.
- Palomino-Vasco, M., Acedo-Valenzuela, M.I., Rodríguez-Cáceres, M.I., Mora-Díez, N., 2019. Automated chromatographic method with fluorescent detection to determine biogenic amines and amino acids. Application to craft beer brewing process. *J. Chromatogr. A* 1601, 155–163. <https://doi.org/10.1016/j.chroma.2019.04.063>.
- Pena-Pereira, F., Wojnowski, W., Tobiszewski, M., 2020. AGREE—analytical greenness metric approach and software. *Anal. Chem.* 92 (14), 10076–11008. <https://doi.org/10.1021/acs.analchem.0c01887>.
- Poveda, J.M., 2019. Biogenic amines and free amino acids in craft beers from the Spanish market: a statistical approach. *Food Control* 95, 227–233. <https://doi.org/10.1016/j.foodcont.2018.09.012>.
- Pranli, T., Moongarm, A., Manwittanakul, G., Loypimai, P., Kerr, W.L., 2021. Melatonin and its derivative contents in tropical fruits and fruit tablets. *J. Food Compos. Anal.* 103, 104109. <https://doi.org/10.1016/j.jfca.2021.104109>.
- Reiter, R.J., Abreu-Gonzalez, P., Marik, P.E., Dominguez-Rodriguez, A., 2020. Therapeutic algorithm for use of melatonin in patients with COVID-19. *Front. Med.* 7 (1), 226. <https://doi.org/10.3389/fmed.2020.00226>.
- Ritota, M., Manzi, P., 2020. Rapid determination of total tryptophan in yoghurt by ultra high performance liquid chromatography with fluorescence detection. *Molecules* 25, 5025. <https://doi.org/10.3390/molecules25215025>.
- Scigalski, P., Kosobucki, P., 2020. Recent materials developed for dispersive solid phase extraction. *Molecules* 25, 4869. <https://doi.org/10.3390/molecules25214869>.
- de Toffoli, A.L., Maciel, E.V.S., Fumes, B.H., Lanças, F.M., 2018. The role of graphene-based sorbents in modern sample preparation techniques. *J. Sep. Sci.* 41, 288–302. <https://doi.org/10.1002/jssc.201700870>.
- Wu, Y., Wang, T., Zhang, C., Xing, X.H., 2018. A rapid and specific colorimetric method for free tryptophan quantification. *Talanta* 176, 604–609. <https://doi.org/10.1016/j.talanta.2017.08.002>.
- Yazdi, A.S., 2011. Surfactant-based extraction methods. *Trends Anal. Chem.* 30, 918–929. <https://doi.org/10.1016/j.trac.2011.02.010>.
- Zeinali, H., Bagheri, H., Monsef-Khoshshesab, Z., Khoshshafar, H., Hajian, A., 2017. Nanomolar simultaneous determination of tryptophan and melatonin by a new ionic liquid carbon paste electrode modified with SnO<sub>2</sub>-Co<sub>3</sub>O<sub>4</sub>@rGO nanocomposite. *Mat. Sci. Eng. C* 71, 386–394. <https://doi.org/10.1016/j.msec.2016.10.020>.
- Zhang, X., Yang, Y., Qin, P., Han, L., Zhu, W., Duan, S., Lu, M., Cai, Z., 2022. Facile preparation of nano-g-C<sub>3</sub>N<sub>4</sub>/UiO-66-NH<sub>2</sub> composite as sorbent for high-efficient extraction and preconcentration of food colorants prior to HPLC analysis. *Chin. Chem. Lett.* 33, 903–906. <https://doi.org/10.1016/j.ccl.2021.07.003>.
- Zolfonoun, E., 2019. Spectrofluorometric determination of L-tryptophan after preconcentration using multi-walled carbon nanotubes. *Anal. Methods Environ. Chem. J.* 2, 43–48. <https://doi.org/10.24200/amecj.v2.i01.43>.